Proc. 6th NZ Geothermal Workshop 1984

A DOWNHOLE GAS SEPARATOR FOR GEOTHERMAL FLUIDS

PART 11: DESIGN OF VORTEX GENERATOR, AND EXPERIMENTAL PRESSURE DROPS IN A MODEL SEPARATOR

J.F. Kanyua* and D.F. Crant-Taylor**

*Geothermal Institute, University of Auckland, New Zealand

**Chemistry Division, DSIR, Wellington, New Zealand

ABSTRACT

The design of the vortex generator, which is the major contributor to the pressure drop across the downhole separator (DHS), is presented. Pressure drop data for the two types of vortex generators used in the model DHS rig at well number BR-22, Broadlands, New Zealand, are also presented.

INTRODUCTION

In part I, the problems associated with occurrence of CO_2 in geothermal fluids and the conceptual design and performance of the downhole separator (DHS) were discussed. Part II covers the design of two types of vortex generators used in the model DHS tested at well number BR-22 in Broadlands, New Zealand. The results of pressure measurements in the various parts of the DHS are presented as a comparison between the performance of the two vortex generators.

Design of the vortex generator

The vortex generator has been identified as the major contributor to the overall pressure drop across the DHS and has therefore received the warranted attention in its design. Flashing in the DHS is undesirable because it increases the mass of steam separated with the non-condensable gases and also because the additional flashing is detrimental to the separation efficiency of the DHS.

Ideally, the vortex generator blades should act as guide blades which alter the direction of flow without expanding the fluids. This requires a design in which the blade passage area remains constant throughout the length of the vortex generator. The blade curvature should be very gradual to avoid sudden changes in flow direction and velocity and also to avoid circulation around the blades, stagnant zones and excessive pressure drop. The blade inlet angle, measured from the plane of the radial axis, should be *90°*. The leading edges should be streamlined to avoid flow separation at the inlet. This may be accomplished by using airfoil-shaped leading edges or alternatively by using thin uniform blades. The latter is preferred due to the ease of fabrication and economy of materials, and has been used in the present work. The area taken up by the hub on which the blades are anchored becomes unavailable for fluid flow and contributes to flow acceleration. The hub diameter should therefore be relatively small, with the leading face of the hub rounded.

The gradual blade curvature calls for a vortex generator of long span. While a slender hub presents no major problem as long as its diameter is sufficient to accommodate all the blades, the long span is undesirable because it increases the overall height of the DHS and frictional losses, and may also present fabrication problems in relation to the hub diameter. A compromise between high performance and overall height of the DHS is therefore required. The blade exit angle and number of blades used are determined by the vortex strength required to segregate the phases within a reasonable height of the separation chamber. Large exit angles, measured from the plane of the radial axis, give high mass throughput but are likely to result in unstable operation due to low centrifugal force to gravity force ratios. On the other hand, small exit angles give high vortex strengths and stability while reducing the mass throughput because of the greater restriction on flow area. Small exit angles reduce the height of the separation chamber requited but may increase the dropwise liquid carry-over mentioned in Part I. In the absence of better knowledge on the flow of two-phase mixtures in vortex generators, the design of the vortex generator relied on past experience in the design of pump and turbine blading.

The two vortex generators used in the experimental DHS at BR-22 are shown on Figures 1 and 2. The first vortex generator (Series A) was constructed using a hub taper angle of 12°, a large end diameter of 64mm, and overall length of 69mm with the leading face spherically rounded as shown on Figure 1. The six blades on this vortex generator are twisted so that a horizontal cross-section at any height of the hub reveals radially arranged blade leading edges. In this fashion, the outer edge of a trailing edge (i.e. at the shroud) has a discharge angle of 45°, with the discharge angle increasing towards the hub. This vortex generator geometry is difficult to make. The second vortex generator (Series B) was constructed to increase whirl and mass throughput, and to simplify the construction difficulties encountered in the design of the Series A vortex generator. The leading edges are arranged radially while the trailing edges are tangential to the hub trailing face with a constant discharge angle of 45°. The blade surface is an arc of a circle as shown on Figure 2. The hub is not tapered, and its leading face is spherically rounded. Series B gives a gradual and uniform change in flow direction, provides a higher initial radial velocity at the trailing edge and also a larger flow area. Figure 2b was used to design the blade for vortex generator B. The hub diameter was fixed at 50mm which is approximately equal to the mean diameter of Series A. The discharge angle, , was chosen to match the minimum discharge angle of Series A, which is 45°, and also in order that the tangential and axial velocity components should be equal or of the same order of magnitude. For the blade to be an arc of a circle of radius r_b, the dimension "a" must be equal to the radius of the hub, i.e. a = 25mm. The resulting height of the hub and the radius of the blade surface are then estimated to be approximately 60mm and 85mm respectively. These dimensions produce a blade with gentle curvature and a vortex generator with a plan view as shown on Figure 2c.

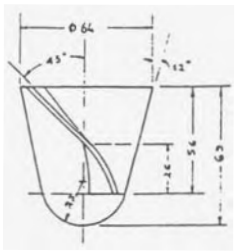

Figure 1 :Vortex generator A : hub and blade detail

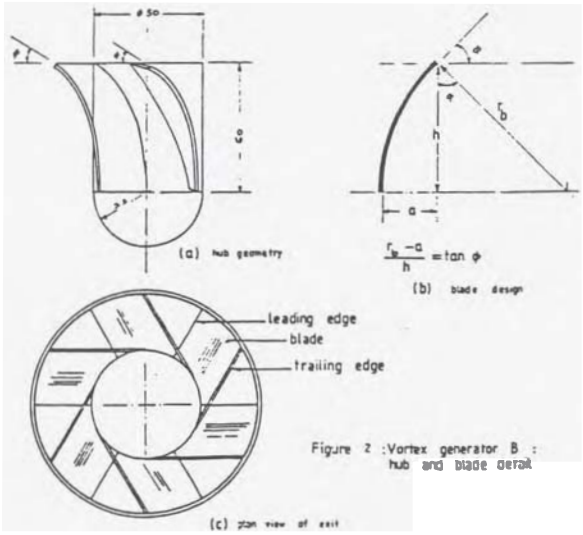

Figure 2 :Vortex generator B : hub and blade detail

Pressure measurements

Figure 3 shows the location and identification of the pressure tappings used and the instrumentation. P_{ref} is the DHS inlet pressure measured by a Bourdon pressure gauge. All the other pressures on the DHS are measured using the above pressure as a reference, i.e. the readings taken indicate the difference between P_{ref} and the local pressure. P_1 is the vortex centre pressure measured from a tapping at the centre of the trailing face of the hub. P_2 and P_3 are pressures in the separation chamber, one above the other. These two tappings are provided with radial traverse probes so that the radial pressure profiles between the chamber wall and the DHS vertical axis may be recorded. The two radial traverses were done at 5mm intervals starting at the wall going to the axis and back. P4 is the DHS exit pressure measured in the separated liquid annulus above the diffuser of the DHS. The full experimental procedure is given in Part III and by Grant-Taylor and Kanyua (1984). The mean P_{ref} was approximately 10.2 bar absolute while the differential pressures have a possible error of about 0.8 kPa (=0.1 psi). Higher precision was made impossible by the level of vibration in the rig and slugging.

Results and Discussion

The pressure drops are plotted as functions of total mass flow rate and vapour mass fraction on Figures 4 to 7. Figure 4 shows the vortex centre relative pressure, $(P_{ref} - P_1)$, as a function of total mass flow rate for fixed vapour mass fractions for both Series A and Series B vortex generators. The vortex centre pressure decreases very rapidly, i.e. $(P_{ref} - P_1)$ increases rapidly with increasing total mass flow rate. The rate at which $(P_{ref} - P_1)$ increases is seen to increase with increasing vapour mass fraction. At a given total mass flow rate and vapour mass fraction Series A gives a much lower vortex centre pressure than Series B. Low values of P_1 may result in flashing in the DHS and therefore increase the vapour

superior to vortex generator A. Figure 5 shows $(P_{ref} - P_1)$ as a function of the vapour mass fraction for fixed total mass flow rates. $(P_{ref} - P_1)$ is seen to be fairly linear with X_V, especially for vortex generator B, as indicated by the linear regression coefficients (lrc) which are given in this figure. Once again, Series A gives lower vortex centre pressures than Series B for the same flow conditions. The slopes of the linear regression lines decrease with decreasing total mass flow rate for both vortex generators.

Figure 6 shovs the total pressure drop as a function of total mass flow rate for fixed vapour mass fractions for both vortex generators. $(P_{ref} - P_4)$ increases rapidly with increasing total mass flow rate. Once again, the superiority of vortex generator B is obvious. Figure 7 shows $(P_{ref} - P_4)$ and $(P_{ref} - P_{2wall})$ plotted against X_V for fixed total mass flow rate for Series B vortex generator. Here P_{2wall} refers to P_2 measured at the separation chamber wall. Both curves are seen to be fairly Linear, and also the difference between $(P_{ref} - P_4)$ and $(P_{ref} - P_{2wall})$ is seen to be small especially at low values of X_V but increasing at higher values of X_V. The similarity between Figure 4 and Figure 6, and Figure 5 and Figure 7, is to be expected because the vortex generator is the major contributor to the total pressure drop, and axial pressure drops in the separation chamber have been shown to be negligible (see Grant-Taylor and Kanyua, 1984). A comparison between $(P_{ref} - P_4)$ and $(P_{ref} - P_{2wall})$ for Series A has been omitted but it is similar to the Series B plots shown on Figure 7. Series A data show much larger values of $(P_{ref} - P_4)$ and $(P_{ref} - P_{2wall})$ and also larger differences between these two pressure drops. The gradients for Series A data are also much steeper.

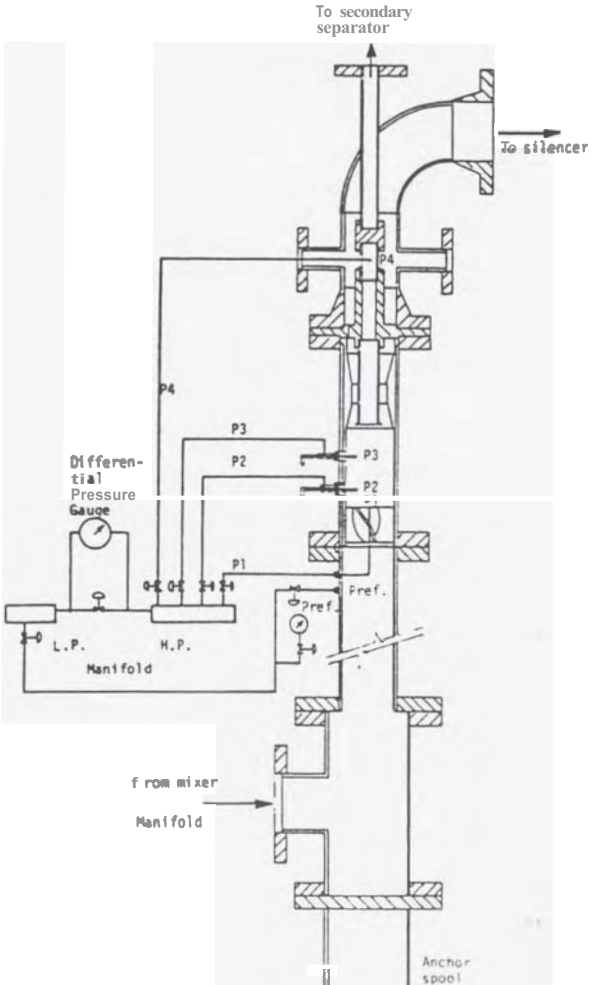

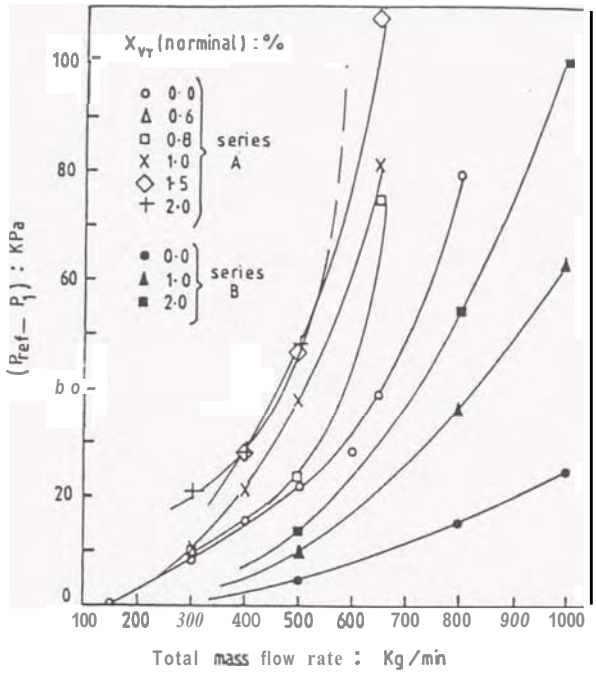

Figure 4 :Vortex centre pressure(relative) as a function of total mass flow rate

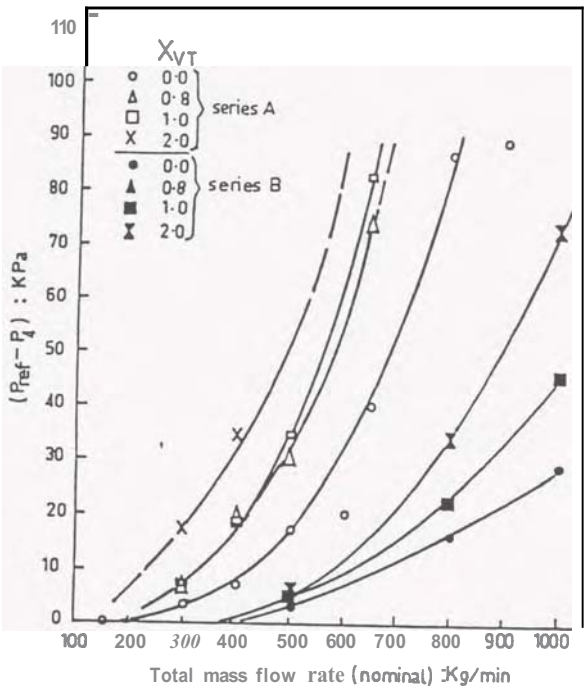

Figure 6 :Total pressure drop across DHS as a function of total mass flow rate

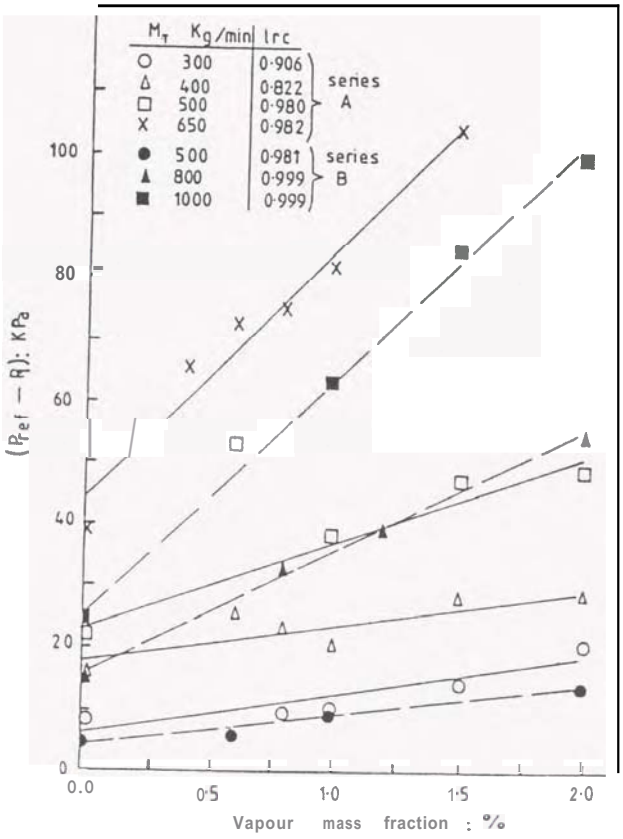

Figure 5 :Vortex centre pressure (relative) as a function of vapour mass fraction

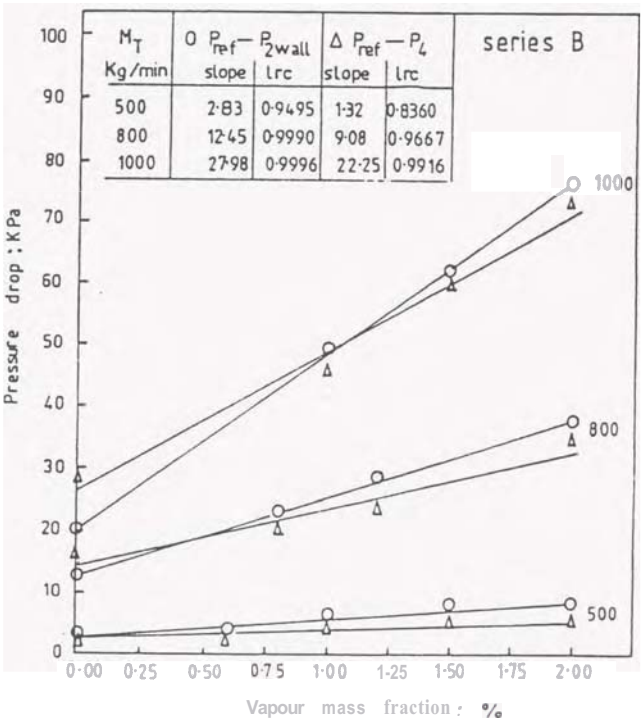

Figure 7 :Total pressure drop & pressure drop across vortex generator as a function of vapour mass traction

The radial pressure profiles have been omitted for brevity. However, it was observed that the pressure remains constant with radius as one moves from the vertical axis of the DHS towards the wall. Close to the wall the profile was observed to attain a maximum at the wall by one of two modes. In the first mode the approach to the wall pressure is monotonic, while in the second mode the pressure drops to a minimum and then increases to the wall pressure. The occurrence of this minimum may indicate the point of changeover from bounded free vortex motion near the wall to solid body rotation or low vortex strength flow associated with bulk of the vapour where the flow direction is predominantly axial.

Conclusions and recommendations

The importance of a properly designed vortex generator has been demonstrated. The superiority of vortex generator B over vortex generator A has been demonstrated. The vortex generator has been shown to contribute practically all the present drop across the DHS. It is also concluded that the diffuser does not accomplish an appreciable pressure recovery and may therefore be omitted in the design of a DXS. The overall pressure drop has been shown to increase very rapidly with increasing total mass flow rate for a given vapour mass fraction. The overall pressure drop has also been shown to be a fairly linear function of vapour mass fraction. The need to locate the DHS at a point where the vapour mass fraction is low, i.e. close to the point of first flashing, has been demonstrated insofar as pressure drop is concerned.

Further improvement in the performance of the vortex generator may be accomplished by optimising the geometry of the vortex generator.

ACKNOWLEDGEMENTS

This project was funded by the Electricity Department, Ministry of Energy, in association with the Chemistry Division of the Department of Scientific and Industrial Research, New Zealand. The assistance provided by the Geothermal Research Centre, Wairakei, and the Ministry of Works and Development is gratefully acknowledged.

REFERENCE

Grant-Taylor, D.F. and Kanyua, J.F., 1980: An experimental downhole separator for removal of geothermal gas; Chem. Div., DSIR, Report (in press).